



Protein-bound calcium phosphate in uremic rat serum: a quantitative study

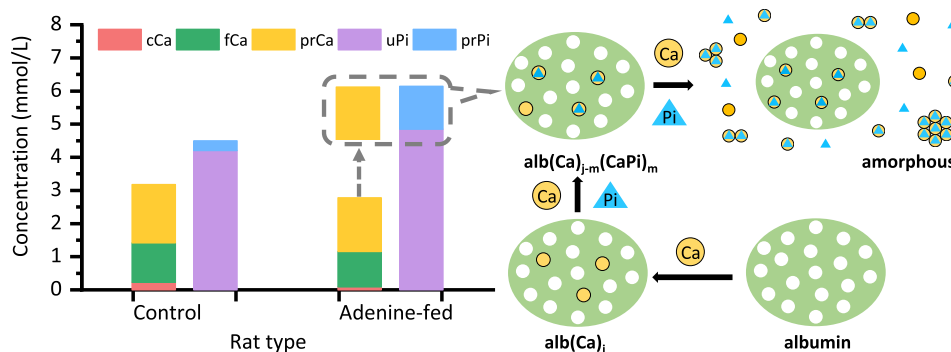
Hong-Xing Fan^{1,2} · Bao-Di Gou³ · Yu-Xi Gao² · Gang Wu¹ · Shu-Hu Liu⁴ · Fan Li⁴ · Tian-Lan Zhang³

Received: 14 April 2020 / Accepted: 4 August 2020 / Published online: 24 August 2020
© Society for Biological Inorganic Chemistry (SBIC) 2020

Abstract

Abstract Protein-bound calcium (prCa) constitutes about 40% of serum total calcium, in which albumin is the most dominant protein. Given the chemical interaction between calcium and phosphate (Pi), the increased serum Pi in chronic kidney disease may cause changes in the composition and structure of the prCa fraction. Here, we report the phosphate binding on the protein-bound calcium in uremic rat serum. Using adenine-fed rats as a uremic model, we separated the calcium and phosphate fractions in rat serum by ultrafiltration, and found that the level of protein-bound phosphate (prPi) in the uremic serum was markedly higher than in control. The elevated prPi level was comparable to the prCa level, consistent with the presence of protein-bound calcium phosphate $\text{pr}(\text{Ca})_{j-m}(\text{CaPi})_m$. We then confirmed its presence by ex vivo X-ray absorption near-edge structure spectroscopy, revealing the discrete state of the calcium phosphate clusters associated with protein. Finally, in a quantitative investigation using Ca- and Pi-boostered serum, we discovered the threshold concentration for the Pi binding on prCa, and determined the binding constant. The threshold, while preventing Pi from binding to prCa in normal condition, allows the reaction to take place in hyperphosphatemia conditions. The protein-bound calcium phosphate could act as a link between the metabolism of serum proteins and the homeostasis of phosphate and calcium, and it deserves further investigation whether the molar ratio of $(\text{prPi}/\text{prCa}) \cdot 100\%$ may serve as a serum index of the vascular calcification status in chronic kidney disease.

Graphic abstract



Keyword Calcium phosphate · Albumin · Serum · Hyperphosphatemia · Threshold concentration

✉ Gang Wu
wugang0525@163.com

✉ Tian-Lan Zhang
tlzhang@bjmu.edu.cn

Extended author information available on the last page of the article

Abbreviations

ACP	Amorphous calcium phosphate
CPPs	Calciprotein particles
CKD	Chronic kidney disease
cCa	Complexed calcium by small anions
DLS	Dynamic light scattering
FMC	Fetuin–mineral complex

FTIR	Fourier transform infrared spectroscopy
fCa	Free calcium
HAP	Hydroxyapatite
prCa	Protein-bound calcium
prPi	Protein-bound phosphate
SAXS	Small-angle X-ray scattering
tCa	Total calcium
TEM	Transmission electron microscopy
uCa	Ultrafilterable calcium
XANES	X-ray absorption near-edge structure

Introduction

Albumin, as the dominant constituent of human serum proteins, markedly affects the distribution of serum calcium. Protein-bound calcium (prCa) makes up about 40% of serum total calcium (tCa), in which albumin accounts for 81% of the bound calcium ions [1]. Because the formation of prCa causes a drop in the level of physiologically active free calcium (fCa), various formulas have been derived to “correct” the clinically determined tCa for changes in albumin [2]. The calcium complexed by small anions (cCa) has a relatively minor effect on fCa, owing to its small proportion (5%–15%) [3]. Equation 1 shows the mass balance of the calcium fractions in serum, where fCa and cCa, together, are frequently referred to as ultrafilterable calcium (uCa):

$$tCa - prCa = uCa = fCa + cCa. \quad (1)$$

The prCa fraction, in addition to mediating serum calcium, is likely involved in phosphate-associated physiology and pathology. Calcium and phosphate (Pi) can form ionic clusters [4], amorphous solid (amorphous calcium phosphate, ACP) [5], and several crystalline phases in aqueous media at near neutral pH, of which the most stable is hydroxyapatite (HAP) [6]. Given the chemical interaction between Ca^{2+} and Pi, the hyperphosphatemia with chronic kidney disease (CKD) may cause phosphate binding on the protein-bound calcium in serum, leading to the formation of protein-bound calcium phosphate. This kind of substance, such as fetuin–mineral complex (FMC) [7] or calciprotein particles (CPPs) [8], has been detected in the serum of CKD patients [9, 10] and uremic model rats [11]. As the major protein in FMC or CPPs, fetuin-A binds to calcium phosphate particles rather than sequesters individual calcium ions like albumin [8]. Note that albumin, while mainly binding calcium ions in normal conditions [12], can also bind calcium phosphate mineral, though less potently [13]. In these cases, both calcium and phosphate contents should be determined to characterize the prCa fraction in serum.

Various techniques have been applied to the characterization of the protein-bound calcium phosphate in blood serum.

As a commonly used uremic animal model, adenine-fed rats recapitulate some features of human CKD, including hyperphosphatemia [14–16]. In 2009, Matsui et al. detected a kind of FMC with the Ca/Pi molar ratio of 1.05 in the pellet of adenine-fed rat serum after centrifugation [11]. In 2017, Smith et al. detected amorphous type-1 and crystalline type-2 CPPs in CKD patients and uremic model rats, using a fluorescent probe-based flow cytometric assay [10]. In 2018, Viegas et al. observed type-1 CPPs (spheroid particles) and type-2 CPPs (needle-like structures) in the control and CKD stage 5 patients, respectively, by transmission electron microscopy (TEM) and micro-Fourier transform infrared spectroscopy (FTIR) [17]. In 2019, Chen et al. assessed the transformation of type-1 to type-2 CPPs in the serum of CKD patients and healthy volunteers using a dynamic light scattering (DLS) assay [18]. And most recently, Akiyama et al. determined the hydrodynamic radii of CPPs in cell culture by small-angle X-ray scattering (SAXS), from which they derived the size and shape of CPPs [19]. However, it remains a challenging task to acquire direct structural information of the protein-bound calcium phosphate, owing to the crystallizing propensity of the calcium phosphate clusters and amorphous phase. Ideally, *ex vivo* techniques should be used in the structural investigation of the prCa fraction, *i.e.*, without any additives and with the least sample-preparation procedure. Among these techniques is X-ray absorption near-edge structure (XANES) spectroscopy. Such a spectrum is sensitive to the short-range order of the target atom, providing information on coordination geometry and bond angles [20]. Additionally, with the application of synchrotron radiation, the signal-to-noise ratio in data collection has been high enough for the *ex vivo* detection of serum calcium [12, 21].

In the present study, we aimed (1) to determine the phosphate contents associated with the calcium fractions in the serum of adenine-fed rats; (2) to characterize the structure of protein-bound calcium in rat serum by *ex vivo* XANES spectroscopy at Ca K-edge; and (3) to investigate the phosphate binding on protein-bound calcium quantitatively, using Ca- and Pi-boosted serum of normal rats.

Materials and methods

Chemicals

$CaCl_2 \cdot 2H_2O$, Na_2HPO_4 , NaCl, hydroxyapatite nanopowder [HAP, $Ca_{10}(PO_4)_6(OH)_2$], and adenine were purchased from Sigma-Aldrich (Saint Louis, MO, USA). Calcium standard (0.1000 ± 0.0005 mol/L, Orion 922,006) was from Thermo (Beverly, MA, USA). Bovine serum albumin (BSA) was the product of J&K Scientific (Beijing, China). High purity HNO_3 was from Beijing Chemical Works (BV-III Grade,

Beijing, China). Other reagents were of analytical grade. Solutions were prepared fresh with deionized and distilled water.

Animals and diet

Male Sprague–Dawley rats (5 week old, 150 g – 180 g) were purchased from Beijing Vital River Laboratory Animal Technology (Beijing, China). The maintaining diet (Beijing Keao Xieli Feed Co., Ltd., Beijing, China) contains 1.0% – 1.8% calcium and 0.6% – 1.2% phosphorus. All experiments involving rats were approved by the Animal Care and Use Committee of Peking University and conformed to the international guidelines on the ethical use of animals.

We used three kinds of rats. (1) Adenine-fed rats: They were purchased and, after one-day acclimatization, were fed the diet containing 0.75% adenine (0.75 g adenine in 100 g of the maintaining diet) for the next 5 weeks. (2) Control rats: They were purchased and fed the maintaining diet for the next 5 weeks. (3) Normal rats: They were purchased and used in the same day, for the preparation of Ca- and Pi-boosted serum. We used these serum samples in the investigation of the Ca–protein binding and Pi binding to the protein-bound calcium.

To make the period shortest between the sample preparation and the spectral data collection, we typically arranged a set of experiments like this: Eighteen normal rats were purchased and randomly allocated into two groups. The control group ($n = 8$) were given the maintaining diet for the next 5 weeks, whereas the adenine-fed group ($n = 10$) were treated with the 0.75% adenine diet for the same period. In the day before the last day of the period, normal rats ($n = 20$) were purchased and used for serum preparation in the same day. At the end of the 5-week period, the adenine-fed and control rats were treated for serum preparation. The spectral data of all serum samples from the normal, control, and adenine-fed rats were collected in the same period of beamtime.

Serum, retentate, and pellet samples

After treatment with diethyl ether, the rats were taken blood from eyes and sacrificed under anesthesia. The typical volumes of the collected blood were 1.0 mL from a normal rat, 1.0 mL from a uremic rat, and 1.4 mL from a control rat,

respectively. The blood was allowed to clot for 30 min at room temperature (circa 25 °C) under anaerobic conditions, and then centrifuged at 2000×g for 15 min in capped plastic tubes. By mixing equal volume of sera from different rats, we prepared pooled sera to make the amount large enough for a set of experiments, including the determination of calcium and phosphate contents, the measurement of fCa and pH, and the preparations of retentate and pellet samples for XANES spectra. Typically, we needed about 8 mL of serum for a set of measurements.

After collecting samples (0.2 mL × 2) for the determination of calcium and phosphate on an AU5800® Chemistry Analyzer (Beckman Coulter, Inc.), we measured the pH of the pooled sera aerobically and adjusted it to 7.35–7.38 with HCl solution on a multi-functional instrument (SevenExcellence™, Mettler Toledo, Switzerland). Then, we measured serum pH and fCa simultaneously, and recorded the fCa reading while the pH value approached to 7.40, using an InLab®MaxPro-ISM electrode with an MT TempSensor for pH and a perfectION™ combination electrode for fCa (Mettler Toledo, Switzerland). The required sample volume is 2.5 mL to immerse the two electrodes. A three-point calibration (4.0, 7.0, 9.0) for pH and a four-point calibration (0.5, 1.0, 2.0, 4.0 mmol/L in 0.9% NaCl) for Ca²⁺ were performed immediately before the measurements.

Ultrafiltration was performed by centrifugation at 5000×g for 50 min (HC-3018, Zhongjia Co., Anhui, China), using Amicon® Ultra 30 K devices with the membrane of 30 kDa cut-off molecular weight (Merck Millipore Ltd., Ireland). Samples were taken from the serum and the ultrafiltrate for the determination of calcium and phosphate (AU5800® Chemistry Analyzer, Beckman Coulter, Inc.). The retentate was kept anaerobically in the device at room temperature for the collection of XANES spectral data within 4 h.

Pellet samples were prepared on a Centrifuge 5810R (Eppendorf AG, Hamburg, Germany) at 16 000×g for 2 h at 25 °C. The supernatant was taken for the determination of calcium and phosphate (AU5800® Chemistry Analyzer, Beckman Coulter, Inc.). The pellet was kept anaerobically in the tube at room temperature for the collection of XANES spectral data within 2 h.

Ca- and Pi-boosted serum: Predetermined volume of CaCl₂ (10 mmol/L in NaCl 0.9%, pH 6.0–7.0) or Na₂HPO₄ (10 mmol/L in NaCl 0.9%, pH 7.0–7.4) solution was added to a portion of the pooled sera from normal rats (3 mL/

Table 1 Calcium and phosphate contents in Ca- and Pi-boosted serum

Specimen	Pi-boosted serum			Serum	Ca-boosted serum		
	S3Pi	S2Pi	S1Pi		S1Ca	S2Ca	S3Ca
tPi	5.16 ± 0.02	4.60 ± 0.08	4.08 ± 0.06	3.54 ± 0.01	3.54*	3.54*	3.54*
tCa	3.08*	3.08*	3.08*	3.08 ± 0.03	3.77 ± 0.06	4.44 ± 0.04	5.24 ± 0.03

Mean ± standard deviation (unit: mmol/L). *Values taken from that for the sample S0

portion, $n=28$). Additional 0.9% NaCl solution was complemented to make the total volume of 3.6 mL/portion. The concentrations of Ca and Pi of these specimens are listed in Table 1.

We filled the space above the liquid in the plastic tubes with CO₂/air mixture, to inhibit the pH rise caused by CO₂ releasing. We then kept these tubes in a water bath at 39 °C (near rat body temperature) for 2 h, and vortexed them at a 15-min interval. At the end of the incubation, we checked and brought the pH of these specimens to 7.35–7.38, followed by the measurement of fCa and ultrafiltration (Amicon® Ultra 30 K devices, Merck Millipore Ltd., Ireland). Samples were taken from the serum specimens and their ultrafiltrates for the determination of calcium and phosphate.

Spectral references

Amorphous calcium phosphate mixed with serum (ACP@serum): This reference was prepared on site by mixing 0.80 mL of solution X (CaCl₂ in 0.9% NaCl, 20 mmol/L, pH 6.0–7.0) and 1.0 mL of solution Y [(8.0 mL of Na₂HPO₄ in 0.9% NaCl, 20 mmol/L, pH 8.87) + (0.60 mL of NaOH 0.1 N)]. The mixture was immediately centrifuged at 5000×g for 2 min. After decanting the supernatant, we mixed the pellet with 4.0 mL of serum and then divided the mixture into two portions. One of them was immediately centrifuged at 10,000×g for 5 min, and the other was centrifuged after 2 h. We removed 1.5 mL of the supernatant with a pipette, stirred the residue with the pipette tip, and, finally, placed the slurry into a sample cell to collect the spectral data.

Hydroxyapatite mixed with serum (HAP@serum): We mixed hydroxyapatite nanopowder with serum (2.0 mg/mL), kept the mixture at room temperature for about 2 h, and vortexed it at a 15-min interval. The HAP precipitate was separated with a mini centrifuge, and placed into a sample cell for the collection of the spectral data.

Retentate of albCa: To 4.0 mL of CaCl₂ (3 mmol/L in 0.9% NaCl, pH 6.0–7.0) was added 0.1603 g of bovine serum albumin, producing a mixture with the albumin concentration of 0.606 mmol/L. The mixture was then kept in a water bath at 39 °C for 4 h, and vortexed at a 15-min interval. At the end of the incubation, we performed ultrafiltration (Amicon® Ultra 30 K devices, Merck Millipore Ltd., Ireland) at 6000×g for 60 min. The retentate was pale yellow in color, and the filtrate was a colorless, clear solution (pH 6.80, fCa = 2.39 mmol/L).

Calcium K-edge XANES spectroscopy

The experiments were conducted on Beamline 4B7A at Beijing Synchrotron Radiation Facility (BSRF), China [21]. Experimental settings and conditions were as previously described [12]. We collected the spectral data in the mode

of partial fluorescence yield. The shape of the light spot was an ellipse (circa 8 mm × 6 mm) on the window of a sample cell that contained 0.18–0.20 mL of liquid sample. To ensure the required level of signal-to-noise ratio and to reduce the effect of fCa on the retentate and pellet samples, we enriched the prCa fraction from 3.0 mL of blood serum each by ultrafiltration and high-speed centrifugation. The data collection of the pellet and retentate samples commenced within 2 h and 4 h, respectively, from the completion of centrifugation.

Results and discussion

We determined the phosphate contents associated with the respective calcium fractions and, thus, found the comparable levels of prPi and prCa in adenine-fed rat serum. We then discovered the discrete state of protein-bound calcium phosphate clusters by *ex vivo* XANES spectroscopy. And finally, with Ca- and Pi-boosted serum of normal rats, we studied the formation of the protein-bound calcium phosphate quantitatively, revealing the presence of a threshold concentration for the phosphate binding on protein-bound calcium.

Calcium and phosphate fractions in rat serum

The 0.75% adenine diet caused uremia in the Sprague–Dawley rats, as evidenced by the dramatic difference between the kidneys of an adenine-fed rat and those of a control rat. The normal kidneys are smaller and dark red in color (Fig. 1, left), whereas those of the adenine-fed rat are larger, grayish white (Fig. 1, right), consistent with the observation by Yokozawa et al. [22]

Listed in Table 2 are the calcium and phosphate contents in rat serum. To our knowledge, this is the first report on the phosphate fractions in blood serum. The markedly elevated level of total phosphate (tPi) is in line with the report by Matsui et al. [11], confirming the presence of hyperphosphatemia in the uremic model rats. Furthermore, the protein-bound phosphate (prPi) is significantly higher in the serum of adenine-fed rats than that in control rats. Along



Fig. 1 Kidneys of control (left) and adenine-fed (right) rats

Table 2 Calcium and phosphate fractions in the serum of SD rats*

Rat type	tCa	tPi	fCa	uCa	uPi	prCa \diamond	prPi \diamond	prPi/prCa	cCa $\#$	fCa%	cCa%	prCa%	Remarks
Adenine-fed, $n=9$	2.78 ± 0.39	6.14 ± 0.21	1.07 ± 0.01	1.16 ± 0.01	4.85 ± 0.04	1.62	1.29	0.80	0.09	38.5	3.24	58.3	This work
	1.87	6.13											Wistar rats, Serum [11]
Control, $n=14$	3.18 ± 0.42	4.50 ± 0.20	1.19 ± 0.10	1.42 ± 0.21	4.20 ± 0.10	1.76	0.30	0.17	0.23	37.4	7.23	55.3	This work
	2.31	2.34											Wistar rats, Serum [11]
	2.50		1.39	1.49		1.01			0.10				SD rats, plasma [24]
	3.08	4.06											SD rats, serum [25]

* Pooled sera, pH adjusted to 7.38–7.40 immediately before fCa measurement and ultrafiltration. Mean ± standard deviation. Four samples were taken from two specimens of pooled sera for the control ($n=6$ and 8) and from one specimen of pooled sera for the adenine-fed ($n=9$) rats, respectively

\diamond Protein-bound (prCa or prPi) = total (tCa or tPi) – ultrafilterable (uCa or uPi)

$\#$ Complexed Ca (cCa) = uCa – free Ca (fCa)

with the elevated phosphate levels, the contents of tCa and its fractions (fCa, uCa, prCa, and cCa) are all lower in the uremic serum than their respective counterparts in the control. The elevated tPi level has been reported to turn more fCa into cCa in patients with end-stage kidney disease [23], but the cCa level found in this study is lower in adenine-fed rats. Some of the previously reported data are also listed in Table 2 for comparison, though none of them contains a complete set of data including both calcium and phosphate fractions.

Protein-bound calcium phosphate in adenine-fed rat serum

The prCa fraction constitutes more than half of tCa in the serum of either adenine-fed or control rats (Table 2). However, its reaction with serum phosphate, along with the possible pathophysiological implications, has rarely been reported. As shown in Table 2, the level of the prPi fraction, low in the serum of control rats, rose to 80% of the prCa fraction in the serum of adenine-fed rats. Since albumin is the dominant protein in prCa [1] and the Pi–albumin interaction is weaker than the Pi–Ca²⁺ interaction, the Pi anions (mainly HPO₄²⁻ at physiological pH [26]) in the prPi fraction bind mainly on the albumin-bound Ca²⁺ cations, leading to the formation of albumin-bound calcium phosphate. We use the formula pr(Ca)_{*j*}–m(CaPi)_{*m*} ($j \geq m$) to denote the composition of the prCa fraction in the adenine-fed rat serum. Notably, the protein-bound Mg²⁺ cations (0.2–0.3 mmol/L [27, 28]) could form similar compound. Given the significant difference between the prPi/prCa molar ratios of the adenine-fed (0.8) and control rats (<0.3), the quantity of (prPi/prCa) · 100% may serve as a serum index of the vascular calcification status in chronic kidney disease.

Calcium phosphate in the pellet and retentate samples from rat serum

To detect the structure of the protein-bound calcium phosphate in the adenine-fed rat serum, we separated it from pooled sera by centrifugation and ultrafiltration, respectively, and characterized the two kinds of samples by Ca K-edge XANES spectroscopy. Shown in Fig. 2a, c are the spectra of pellet and retentate samples, respectively. The structural information can be attracted from a spectrum by comparing it with those of known structures, the “fingerprinting method” [29]. We used fCa as the basic reference for all serum samples, because hydrated Ca²⁺ cations have the known structure and fCa is the simplest of all calcium fractions. Additional references are those that have known structures and exhibit similar spectra to the respective samples (Fig. 2b, d).

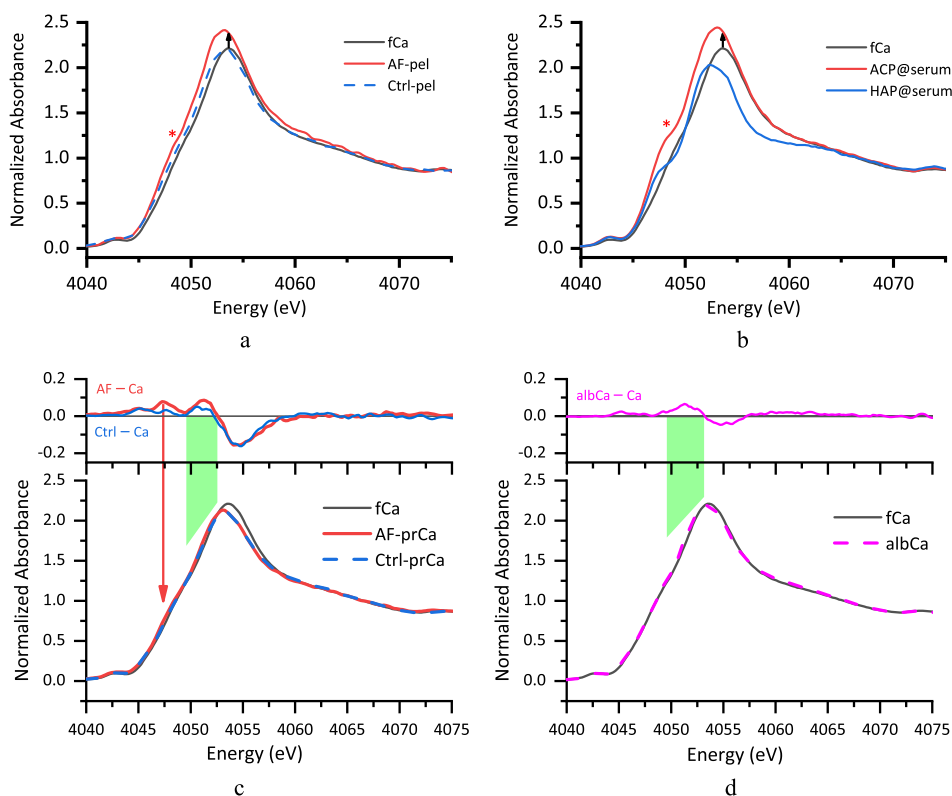


Fig. 2 Ca K-edge X-ray absorption spectra of the protein-bound calcium in rat serum and references. **(a)** Pellet samples separated from the serum of adenine-fed (AF-pel, $n=3$) and control (Ctrl-pel, $n=4$) rats by centrifugation; **(b)** pellet samples of references: Nanocrystalline hydroxyapatite (HAP@serum) and as-made amorphous calcium phosphate (ACP@serum) mixed with serum and separated by centrifugation; **(c)** protein-bound calcium (AF-prCa, $n=10$; Ctrl-prCa,

$n=7$) as retentate samples separated by ultrafiltration; **(d)** retentate sample separated from of albumin–CaCl₂ solution (albCa) by ultrafiltration. In the upper parts of **(c)** and **(d)**, difference spectra are presented to facilitate the analyses. The spectrum fCa, included in all panels as a basic reference, is an average of 22 traces of the CaCl₂ solutions (4 of 50 mmol/L, 12 of 12 mmol/L, and 6 of 6.0 mmol/L) from four beamtimes

The spectrum of the pellet sample from adenine-fed rat serum (AF-pel, Fig. 2a) bares close resemblance to the spectrum of ACP mixed with serum (ACP@serum, Fig. 2b). Both of them exhibit intensified and slightly left-shifted main peaks, as compared with the basic reference fCa. Additionally, both of them exhibit the shoulders on the left side of their main peaks. These spectral features are much less prominent in the spectrum of the control sample (Ctrl-pel, Fig. 2a). The shoulder and the main peak have been attributed to the electron transitions of $1s \rightarrow 4s$ and $1s \rightarrow 4p$, respectively [30]. The left shift of the main peak indicates a reduced effective charge on the Ca atom due to anion-binding, assuming that the sample (AF-pel or ACP@serum) and its reference (fCa) are similar in the coordination geometry of their Ca atoms [31]. And the emergence of the shoulder may result from the bidentate-binding mode [12], in addition to the sixfold coordination geometry [32]. In the presence of the hyperphosphatemia with adenine-fed rats, HPO₄²⁻ was the most abundant bidentate ligand. Its binding on a hydrated Ca²⁺ ion led to the formation of Ca(η^2 -HPO₄)

(H₂O)₄ (where η^2 indicates the bidentate-binding mode) with the association constant $K=390$ at 37 °C [33], accounting for the shoulder at 4047.5 eV [5, 12]. Because AF-pel and ACP@serum share these common spectral features, the short-range structures around the Ca atoms should be same in the two samples. Hence, the calcium species in the pellet from the adenine-fed rats was ACP, and the structure of ACP has been described previously [5]. Crystalline HAP, with the highly reduced intensity and the greater left-shift of the main peak (HAP@serum, Fig. 2b), was unlikely present in the sample AF-pel, though it has been detected in CKD patients by other investigators [10]. By the way, calcium hydrogen carbonate, a constituent of cCa [12, 34], could not exist in the pellet in any appreciable amount, owing to the lower stability of its solution cluster (CaHCO₃⁺, with the association constant $K=10^{1.17}=14.8$ at 35 °C [35]) and the inhibitive effect of phosphate on the formation of amorphous calcium carbonate [36, 37].

We used difference spectra in the analysis of retentate samples. The spectrum of the prCa fraction of adenine-fed

rats (AF-prCa, Fig. 2c) is different with albCa (Fig. 2d) in that the latter lacks the shoulder around 4047.5 eV, confirming the presence of the bidentate-binding mode between Ca^{2+} and HPO_4^{2-} in AF-prCa. On the other hand, the spectrum AF-prCa is similar to AF-pel (Fig. 2a), in view of the left shift of the main peak (green shade) and the presence of the shoulder (arrow) on its left side. These common spectral features indicate the similar structure of AF-prCa and AF-pel. However, the intensity of the main peak is remarkably lower in AF-prCa than that in AF-pel. This spectral difference may reflect the structural difference in the outer sphere of the Ca atoms. Previously, we observed the drop and rebound of the main peak upon mixing calcium and phosphate solutions, and attributed the two spectral features to the formation of the solution clusters $\text{Ca}(\eta^2\text{-HPO}_4)(\text{H}_2\text{O})_4$ and their aggregates, respectively [5]. The hydration degree of CaHPO_4 is higher in solution (sucCa4P6a in Fig. 1a, ref [5].) than in aggregates (sucCa4P6b in Fig. 1a, ref [5].). Judged by the similar spectral features of the aggregates (sucCa4P6b) and the retentate (AF-prCa, Fig. 2c), the calcium phosphate clusters exhibit similar hydration degree in the two cases. However, their stabilities are quite different: The aggregates rapidly developed into ACP, whereas the calcium–phosphate clusters were stable in the serum retentate. Therefore, the calcium–phosphate clusters in the latter case must be in a discrete state predetermined by the discrete Ca^{2+} cations bound on the protein. The interaction between the protein and calcium phosphate clusters, while reducing the hydration degree of both sides, retarded the aggregation of calcium phosphate clusters in $\text{pr}(\text{Ca})_{j-m}(\text{CaPi})_m$. Taking into consideration both the hydration extent and the stability, we conclude that the spectrum of the retentate (AF-prCa, Fig. 2c) represents the discrete calcium phosphate clusters associated with albumin. Again, these spectral features are less significant in Ctrl-prCa than those in AF-prCa (Fig. 2c), demonstrating the effect of the elevated phosphate level on the prCa fraction of adenine-fed rats. To check if ACP passed through the ultrafilter membrane, we took the ultrafiltrate for centrifugation and did not find ACP in the pellet.

Here, we note the use of bovine albCa as a substitute of rat albCa (Fig. 2d). Serum albumins from different species may be different in structure and binding properties [38–40]. According to a recent report, BSA and RSA exist as monomers and multimers, respectively [41]. The two proteins are considerably different in binding some organic ligands [42, 43]. Likewise, their calcium-binding capacity may be different. However, the unspecific binding mode, as revealed in the following discussion, would be same in the two cases. It is the binding mode, rather than the binding capacity, that determines the spectral features of albCa. In this regard, there may not be any significant difference between the spectra of bovine albCa and rat albCa.

The discrete state of the CaPi clusters in $\text{pr}(\text{Ca})_{j-m}(\text{CaPi})_m$ may be of significance in the homeostasis of calcium and phosphate. For example, serum albumin sequesters Ca^{2+} cations in normal conditions, and the generated $\text{pr}(\text{Ca})_j/\text{pr}$ couple plays a role in maintaining the fCa level in serum, much like a weak acid/base couple as a pH buffer [44]. Whereas in pathological conditions with elevated Pi levels, Pi anions bind on the albumin-bound Ca^{2+} cations, thus reducing the Pi excess. As to the ACP detected in the pellet sample, it could be a consequence of centrifugation that caused the discrete clusters to aggregate and develop into ACP (AF-pel, Fig. 2a).

Calcium binds to serum protein

Using a series of Ca- and Pi-boosted serum of normal rats, we studied the formation of protein-bound calcium and protein-bound calcium phosphate. Equation 2 shows the reaction between a Ca^{2+} cation and one of the protein-binding sites (prBS). Equation 3 is the relevant equilibrium equation. Since we use t and j to represent the total number and the occupied number of binding sites per protein molecule, respectively, the equilibrium concentration of prCa is $j \cdot [\text{pr}]$ that corresponds to the compositional formula of $\text{pr}(\text{Ca})_j$:



$$K_j = \frac{[\text{prCa}]}{[\text{prBS}] \cdot [\text{Ca}^{2+}]} = \frac{[\text{prCa}]}{(t \cdot [\text{pr}] - [\text{prCa}]) \cdot \text{fCa}} \quad (3)$$

We transform Eq. 3 into Eq. 4, where fCa and [prCa] were determined experimentally, whereas t and the protein content [pr] are invariants under the experimental condition:

$$\frac{1}{[\text{prCa}]} = \frac{1}{k_j \cdot t \cdot [\text{pr}]} \cdot \frac{1}{\text{fCa}} + \frac{1}{t \cdot [\text{pr}]} \quad (4)$$

Shown in Fig. 3a is the $1/[\text{prCa}]$ versus $1/\text{fCa}$ plot according to Eq. 4. The values of t and K_j can be determined from the intercept and slope by Eqs. 5 and 6, respectively:

$$t = (1/\text{intercept})/[\text{pr}] \\ = (1/103)/(0.63610^{-3} \cdot 0.83) = 18.4 \approx 18 \quad (5)$$

$$K_j = \text{intercept}/\text{slope} = 103/0.696 = 148 \quad (6)$$

where the number 0.83 (= 3.0 mL serum/3.6 mL Ca- or Pi-boosted serum) accounts for the dilution effect resulted from the addition of calcium or phosphate solutions to serum, and the protein concentration [pr] (= 0.636×10^{-3} mol/L)

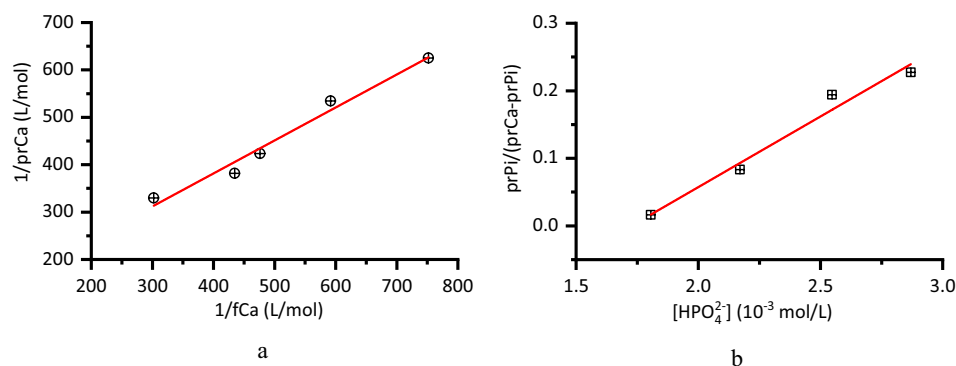


Fig. 3 Correlation of protein-bound fractions with free calcium and phosphate in serum. Pooled sera from normal rats, $n=28$. **a** Formation of prCa. A plot according to Eq. 4. Derived from the linear fitting: Intercept = 103 ± 33.5 , slope = 0.696 ± 0.063 , $R^2 = 0.9681$.

is calculated using the reported values of the molecular weight (64.6 kDa) [45] and the albumin content in control rats (41.1 g/L) [11].

Both specific [46, 47] and non-specific [48] binding modes have been reported between albumin and calcium ions. The specific mode is associated with the fewer binding sites (e.g., $t = 3$ [46]), whereas the number of the non-specific binding sites is usually larger. The values of t and K_j determined in this work ($t \approx 18$ and $K_j = 148$ for rat serum albumin) are comparable to those reported by Pedersen ($t = 13$ and $K = 77$ for bovine serum albumin, $t = 12$ and $K = 100$ for human serum albumin) [49], in line with the non-specific binding. It is worth mentioning that we used complete serum in the determination of t and K , rather than the aqueous solution of purified albumin. Therefore, the higher t and K values are relevant to the higher viscosity of the biological medium. In the serum of control rats, the average number of occupied sites per protein molecule j ($= 2.8$) is about 1/6 of the total binding number t . Here, the value of j is estimated from prCa ($= 1.76$, control rats, Table 2) and the protein concentration [pr] ($= 0.636 \times 10^{-3}$). The number of the binding sites would be higher in a hypercalcemia condition.

Phosphate binds on protein-bound calcium

Equation 7 represents the reaction between serum phosphate and protein-bound calcium, where Pi refers to HPO_4^{2-} . We use m to represent the average number of phosphate bound to the Ca^{2+} ions on a protein molecule, such that the compositional formula of prCaPi is $\text{pr}(\text{Ca})_{j-m}(\text{CaPi})_m$. The relevant equilibrium equation is Eq. 8a that turns to Eq. 8b after rearrangement, where $[\text{prCa}] - [\text{prPi}]$ ($= j \cdot [\text{pr}] - m \cdot [\text{pr}]$) represents the protein-bound calcium ions without phosphate. The produced protein-bound calcium phosphate accounts

b Formation of prCaHPO₄. A plot according to Eq. 8b, in which prCa and prPi stand for protein-bound Ca^{2+} and protein-bound CaHPO_4 , respectively. Derived from the linear fitting: Intercept = -0.361 ± 0.057 , slope = 209 ± 24 , and $R^2 = 0.9618$

for the comparable contents of prPi and prCa in the serum of adenine-fed rats (prPi/prCa = 0.8, Table 2):

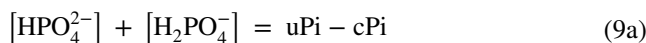


$$K_m = \frac{[\text{prCaPi}]}{([\text{prCa}] - [\text{prCaPi}]) \cdot [\text{HPO}_4^{2-}]}$$

$$= \frac{[\text{prPi}]}{([\text{prCa}] - [\text{prPi}]) \cdot [\text{HPO}_4^{2-}]} \quad (8a)$$

$$\frac{[\text{prPi}]}{([\text{prCa}] - [\text{prPi}])} = K_m [\text{HPO}_4^{2-}]. \quad (8b)$$

On the left side of Eq. 8b, prCa and prPi were experimentally determined. On the right side, the value of $[\text{HPO}_4^{2-}]$ was determined according to Eq. 9, where $K_{a2} = 10^{-7.21} = 6.17 \times 10^{-8}$ [50] and $[\text{H}^+] = 10^{-7.4}$ mol/L as controlled in the experiment. Assuming that the phosphate content in the cPi fraction is equal to the cCa content (Eq. 10), we obtain Eq. 11, where the quantities on the right side (uPi, uCa, and fCa) were directly measured. Now, we could plot $\frac{[\text{prCaPi}]}{([\text{prCa}] - [\text{prCaPi}])}$ against $[\text{HPO}_4^{2-}]$ according to Eq. 8b (Fig. 3b):



$$[\text{HPO}_4^{2-}] = \frac{k_{a2}(\text{uPi} - \text{cPi})}{[\text{H}^+] + K_{a2}}$$

$$= \frac{(6.17 \times 10^{-8})(\text{uPi} - \text{cPi})}{(3.98 + 6.17) \cdot 10^{-8}} = 0.608 (\text{uPi} - \text{cPi}) \quad (9b)$$



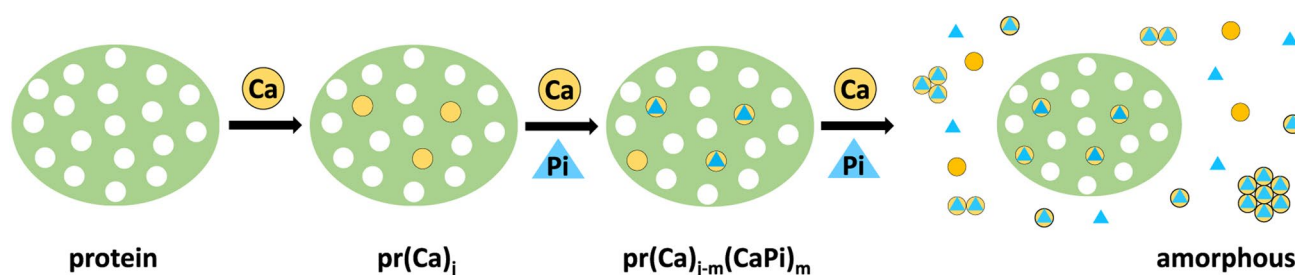


Fig. 4 Two-dimensional schematic of the formation of protein-bound calcium phosphate. $\text{Pi} = \text{HPO}_4^{2-}$. The average numbers of Ca^{2+} and Pi on a protein molecule are designated as j and m , respec-

tively. Note that the value of j , expressed as an integer, is higher in $\text{pr}(\text{Ca})_{j-m}(\text{CaPi})_m$ than in $\text{pr}(\text{Ca})_j$. The protein shape is based on the $11 \text{ nm} \times 8.5 \text{ nm}$ oblate ellipsoid of human serum albumin [56]

$$[\text{HPO}_4^{2-}] = 0.608(\text{uPi} - \text{uCa} + \text{fCa}). \quad (11)$$

From a linear fitting displayed in Fig. 3b, we obtain the binding constant $K_m = \text{slope} = 209 \pm 24$. To our knowledge, the constant of HPO_4^{2-} binding on protein-bound Ca^{2+} (Eq. 7) has never been reported before. The value determined in this work is much lower than those (390 [33], 548 [51], and 681 [52]) determined in aqueous solution without protein, consistent with the reduced positive charge on a protein-bound Ca^{2+} ion. Using the data in Table 2 ($\text{prCa} = 1.62 \text{ mmol/L}$, adenine-fed) and the protein content in the serum of adenine-fed rats (32.4 g/L [11], i.e., 0.502 mmol/L), we obtain $j = 3.2$ and $m = 2.6$, corresponding to a mixture of $\text{pr}(\text{CaPi})_3$ and $\text{pr}(\text{Ca})(\text{CaPi})_2$. In addition to the elevated tCa/albumin ratio, the alteration in the post-translational modifications of the protein in CKD [53, 54] may also be a course for the increased number of protein-bound calcium in the serum of adenine-fed rats. Based on above discussion, the stepwise formations of $\text{pr}(\text{Ca})_j$ and $\text{pr}(\text{Ca})_{j-m}(\text{CaPi})_m$ are depicted in Fig. 4. It is worth noting that, in worsening conditions, CaPi clusters could form out of protein and get aggregated, leading to the formation of amorphous solid (Right, Fig. 4). It is such calcium–phosphate entities that could contribute directly to the vascular calcification in CKD. In this circumstance, serum fetuin-A is more efficient in binding mineral particles, in the form of FMC [11] or CPP-I [9, 10]. In such a colloidal particle, a fetuin-A molecule sequesters 90–120 Ca^{2+} cations and 54–72 Pi anions [8], retarding the crystal growth and regulating mineral trafficking [10, 55]. Thus, the formation of FMC facilitates the clearance and metabolism of insoluble calcium phosphates [9]. In this regard, $\text{pr}(\text{Ca})_{j-m}(\text{CaPi})_m$ and FMCs act as two adjacent links in the chain of events resisting vascular calcification with CKD.

Also derived from the linear fitting in Fig. 3b is the intercept ($= -0.361 \pm 0.057$), according to which we rewrite Eq. 8b as Eq. 12. To reveal the physical meaning of the intercept, we express Eq. 12 as Eq. 13a, where $[\text{HPO}_4^{2-}]_0$ is defined in Eq. 14. Judged on Eq. 13a, the prerequisite for $[\text{prPi}] > 0$ is defined by Eq. 15, where the subscript in $[\text{HPO}_4^{2-}]_0$ represents the “threshold concentration” for

HPO_4^{2-} binding on the protein-bound Ca^{2+} ions, i.e., no HPO_4^{2-} would bind to $\text{pr}(\text{Ca})_j$ if $[\text{HPO}_4^{2-}] \leq [\text{HPO}_4^{2-}]_0$. To make the use of the threshold concept more convenient, we express $[\text{HPO}_4^{2-}]_0$ in terms of the ultrafiltrate fraction (uPi) that can be experimentally determined. From $[\text{HPO}_4^{2-}]/[\text{H}_2\text{PO}_4^-] = K_{a2}/[\text{H}^+] = 10^{-7.21}/10^{-7.40} = 1.55$, we obtain $[\text{H}_2\text{PO}_4^-]_0 = [\text{HPO}_4^{2-}]_0/1.55 = 1.73/1.55 = 1.12 \text{ mmol/L}$. Thus, the threshold of phosphate is: $(\text{uPi})_0 = [\text{HPO}_4^{2-}]_0 + [\text{H}_2\text{PO}_4^-]_0 + \text{cPi} = 1.73 + 1.12 + \text{cPi} \approx 3.0 \text{ mmol/L}$, assuming $\text{cPi} \approx 0.15 \text{ mmol/L}$:

$$\frac{[\text{prPi}]}{([\text{prCa}] - [\text{prPi}])} = K_m[\text{HPO}_4^{2-}] + \text{intercept} \quad (12)$$

$$\frac{[\text{prPi}]}{([\text{prCa}] - [\text{prPi}])} = K_m([\text{HPO}_4^{2-}] - [\text{HPO}_4^{2-}]_0) \quad (13a)$$

$$\frac{[\text{prPi}]}{([\text{prCa}] - [\text{prPi}]) \cdot ([\text{HPO}_4^{2-}] - [\text{HPO}_4^{2-}]_0)} = K_m \quad (13b)$$

$$[\text{HPO}_4^{2-}]_0 \equiv -\text{Intercept}/K_m \\ = 0.361/209 = 1.7310^{-3} \text{ mol/L} \quad (14)$$

$$[\text{HPO}_4^{2-}] - [\text{HPO}_4^{2-}]_0 > 0 \quad (\text{for } [\text{prPi}] > 0). \quad (15)$$

High serum phosphate levels have been linked to higher risks of mortality in CKD [57], and the formation of $\text{pr}(\text{Ca})_{j-m}(\text{CaPi})_m$ could correlate the metabolism of serum proteins with the homeostasis of phosphate and calcium. For example, the Pi -to- $\text{pr}(\text{Ca})_j$ binding would be minor if the serum phosphate level is not too high. However, the binding reaction (Eq. 7) would take place if the level of serum phosphate exceeds the threshold value. Judged by the binding capacity for Pi ($\text{prPi} = 1.29 \text{ mmol/L}$, adenine-fed, Table 2), this mechanism could account for the diurnal variation of tPi after dietary intake [58, 59]. While serum albumin is cleared from circulation via endocytosis by endothelial cells [60, 61],

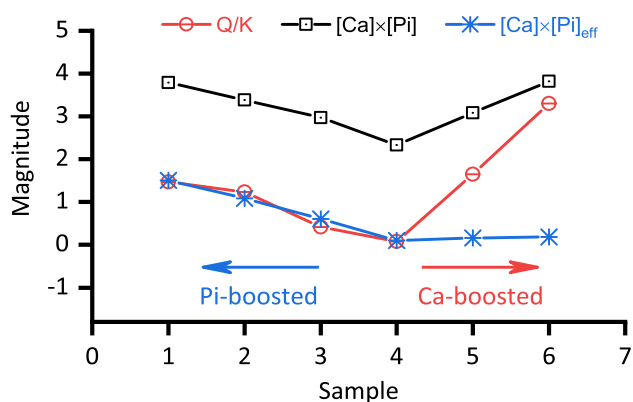
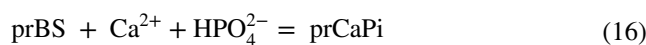


Fig. 5 Variations of $[\text{Ca}] \times [\text{Pi}]$ and $[\text{Ca}] \times [\text{Pi}]_{\text{eff}}$ as compared with Q/K in the phosphate- and calcium-boosted serum. Pi represents HPO_4^{2-} that is determined from Eq. 11. $[\text{Pi}]_{\text{eff}}$ is defined by Eq. 18. The products $[\text{Ca}] \times [\text{Pi}]$ and $[\text{Ca}] \times [\text{Pi}]_{\text{eff}}$ have the unit of $(10^{-3} \text{ mol/L})^2$. Q/K is dimensionless

the associated calcium phosphate clusters $(\text{CaPi})_m$ could be taken away, thus retarding the increase in the level of serum phosphate in the early stages of CKD ($\text{prPi}/\text{prCa} \leq 1$); after all, hyperphosphatemia is noted in the late stages of CKD [62]. When serum albumin molecules are fully loaded, calcium phosphate clusters could emerge out of protein (Right, Fig. 4). More readily, such clusters develop into amorphous calcium phosphate via aggregation-facilitated crosslinking [63] and are cleared from circulation by macrophages [64] and smooth muscle cells [65] in the form of calciprotein particles. A mineral buffering system has been suggested in the blood [66]. Moreover, the relevant tissues (bone, kidney, and intestine) also take actions to maintain the serum phosphate level. Hence, the formation of $\text{pr}(\text{Ca})_{j-m}(\text{CaPi})_m$ might be an early, local, event in the “blood mineral buffering system [66]”. Note that the situation could be different with human, in which the serum phosphate level is much lower. According to a recent report, the upper limit of the serum phosphate associated with the minimum risk of mortality is 5.7 mg/dL (1.84 mmol/L) in post-weekend blood samples [57]. Therefore, it remains to be examined whether the threshold concept is applicable to human, especially the CKD patients with hyperphosphatemia.

Overall reaction: correlation between protein-bound calcium phosphate and $\text{Ca} \times \text{Pi}$

Equation 16 represents the overall reaction that combines the two stepwise reactions (Eqs. 2 and 7). The relevant equilibrium equation (Eq. 17a) is obtained by multiplying Eqs. 3 and 13b. By defining the effective concentration $[\text{HPO}_4^{2-}]_{\text{eff}}$ (Eq. 18) and the quotient Q (Eq. 19), we rewrite Eqs. 17a as 17b:



$$K = K_j K_m = \frac{[\text{prCa}]}{([\text{t} \cdot \text{pr}] - [\text{prCa}])} \cdot \frac{[\text{prPi}]}{([\text{prCa}] - [\text{prPi}])} \cdot \frac{1}{[\text{Ca}] \cdot ([\text{HPO}_4^{2-}] - [\text{HPO}_4^{2-}]_{\text{eff}})} \quad (17a)$$

$$[\text{Ca}^{2+}][\text{HPO}_4^{2-}]_{\text{eff}} = Q/K. \quad (17b)$$

$$[\text{HPO}_4^{2-}]_{\text{eff}} \equiv [\text{HPO}_4^{2-}] - [\text{HPO}_4^{2-}]_0 \quad (18)$$

$$Q \equiv \frac{[\text{prCa}]}{([\text{t} \cdot \text{Pr}] - [\text{prCa}])} \cdot \frac{[\text{prPi}]}{([\text{prCa}] - [\text{prPi}])} \quad (19)$$

Equation 17b reveals the correlation between protein-bound calcium phosphate and the $[\text{Ca}^{2+}] \times [\text{HPO}_4^{2-}]_{\text{eff}}$ product. As displayed in Fig. 5, the $[\text{Ca}^{2+}] \times [\text{HPO}_4^{2-}]_{\text{eff}}$ product increases with increasing tPi, consistent with Q/K in the normal and Pi-boosted serum. However, it is almost invariant in the tCa range of 3.08–4.44 mmol/L (Ca-boosted serum, tPi = 3.54 mmol/L), because the effect of tCa increase is minified by multiplying a small value of $[\text{HPO}_4^{2-}]_{\text{eff}}$. The product $[\text{Ca}] \times [\text{Pi}]$ is also plotted in Fig. 5 for comparison, which increases with either increasing tPi (Pi-boosted serum) or increasing tCa (Ca-boosted serum), reaching a minimum at the “raw serum”. Clinically, the $\text{Ca} \times \text{Pi}$ product is used as a relevant tool in the assessment of the cardiovascular risk [67] associated with the high serum phosphate level in CKD. A target $\text{tCa} \times \text{tPi}$ level of $55 \text{ mg}^2/\text{dL}^2$ has been recommended for evaluating the risks associated with the elevated phosphorus level in dialysis patients [68]. Besides, some experts have suggested replacing tCa with other quantities, such as the albumin-corrected $\text{tCa} \times \text{tPi}$ of $4.0 (\text{mmol/L})^2$ [69] and $\text{fCa} \times \text{tPi}$ of $2.2 (\text{mmol/L})^2$ [67]. Anyway, $\text{fCa} \times [\text{HPO}_4^{2-}]$, as the basis of other forms of the $\text{Ca} \times \text{Pi}$ product, is correlated with the protein-bound calcium phosphate. Using the data in Table 2, the calculated values of $\text{fCa} \times \text{uPi}$ are 5.0 and 5.2 $(\text{mmol/L})^2$ for the control and adenine-fed rats, respectively, and their corresponding $\text{tCa} \times \text{tPi}$ values are 14.3 and 17.1 $(\text{mmol/L})^2$. An elevated $\text{tCa} \times \text{tPi}$ level has been observed in adenine-fed rat serum (140 versus ca $80 \text{ mg}^2/\text{dL}^2$ in control) [15], but no direct comparison can be made due to the use of different units.

Conclusions

Protein-bound calcium phosphate, with the formula of $\text{pr}(\text{Ca})_{j-m}(\text{CaPi})_m$, formed in the serum of uremic rats. Characterized by the threshold concentration of free phosphate and the discrete state of calcium phosphate clusters, the formation of $\text{pr}(\text{Ca})_{j-m}(\text{CaPi})_m$ could act as a link between the metabolism of serum proteins and the homeostasis of phosphate and calcium. It deserves further investigation whether the molar ratio of $(\text{prPi}/\text{prCa}) \cdot 100\%$ may serve as a serum index of the vascular calcification status in the progression of chronic kidney disease.

Acknowledgements This work was supported by the joint funding from the Natural Science Foundation of China and the Chinese Academy of Sciences (No. U1632105), and by the provision of beamtimes of Beijing Synchrotron Radiation Facility at 4B7A. We thank Kun Tang, Lei Zheng, and Yi-Dong Zhao at 4B7A for their guidance in the collection and analyses of the spectral data.

Author contributions H-XF took part in all experiments and the spectral data reduction. B-DG and Y-XG were responsible for the establishment of uremic rat model and guided the pre-analytical treatment of serum samples. FL and S-HL were responsible for the experimental settings of spectral data collection. GW and T-LZ designed the research and collected the spectral data. T-LZ analyzed results and wrote the manuscript. All authors took part in revising and approved the final version.

Compliance with ethical standards

Conflict of interest The authors declare that they have no conflict of interest.

References

- Moore EW (1970) Ionized calcium in normal serum, ultrafiltrates, and whole blood determined by ion-exchange electrodes. *J Clin Invest* 49(2):318–334. <https://doi.org/10.1172/jci106241>
- Dickerson R, Alexander K, Minard G, Croce M, Brown R (2004) Accuracy of methods to estimate ionized and "corrected" serum calcium concentrations in critically ill multiple trauma patients receiving specialized nutrition support. *J Parenteral Enteral Nutr* 28(3):133–141. <https://doi.org/10.1177/0148607104028003133>
- Morton AR, Garland JS, Holden RM (2010) Reviews: Is the calcium correct? Measuring serum calcium in dialysis patients. *Semin Dial* 23(3):283–289. <https://doi.org/10.1111/j.1525-139X.2010.00735.x>
- Du L-W, Bian S, Gou B-D, Jiang Y, Huang J, Gao Y-X, Zhao Y-D, Wen W, Zhang T-L, Wang K (2013) Structure of clusters and formation of amorphous calcium phosphate and hydroxyapatite: from the perspective of coordination chemistry. *Cryst Growth Des* 13(7):3103–3109. <https://doi.org/10.1021/cg400498j>
- Zhang Q, Jiang Y, Gou B-D, Huang J, Gao Y-X, Zhao J-T, Zheng L, Zhao Y-D, Zhang T-L, Wang K (2015) In situ detection of calcium phosphate clusters in solution and wet amorphous phase by synchrotron X-ray absorption near-edge spectroscopy at calcium K-edge. *Cryst Growth Des* 15(5):2204–2210. <https://doi.org/10.1021/cg5018505>
- Wang L, Nancollas GH (2008) Calcium orthophosphates: Crystallization and dissolution. *Chem Rev* 108:4628–4669
- Price PA, Thomas GR, Pardini AW, Figueira WF, Caputo JM, Williamson MK (2002) Discovery of a high molecular weight complex of calcium, phosphate, fetuin, and matrix γ -carboxyglutamic acid protein in the serum of etidronate-treated rats. *J Biol Chem* 277(6):3926–3934. <https://doi.org/10.1074/jbc.M106366200>
- Heiss A, DuChesne A, Denecke B, Grotzinger J, Yamamoto K, Renne T, Jahnhen-Dechent W (2003) Structural basis of calcification inhibition by α 2-HS glycoprotein/fetuin-A. *J Biol Chem* 278(15):13333–13341
- Smith ER, Hewitson TD, Hanssen E, Holt SG (2018) Biochemical transformation of calciprotein particles in uraemia. *Bone* 110:355–367. <https://doi.org/10.1016/j.bone.2018.02.023>
- Smith ER, Hewitson TD, Cai MMX, Aghagolzadeh P, Bachtler M, Pasch A, Holt SG (2017) A novel fluorescent probe-based flow cytometric assay for mineral-containing nanoparticles in serum. *Sci Rep* 7(1):5686. <https://doi.org/10.1038/s41598-017-05474-y>
- Matsui I, Hamano T, Mikami S, Fujii N, Takabatake Y, Nagasawa Y, Kawada N, Ito T, Rakugi H, Imai E, Isaka Y (2009) Fully phosphorylated fetuin-A forms a mineral complex in the serum of rats with adenine-induced renal failure. *Kidney Int* 75(9):915–928. <https://doi.org/10.1038/ki.2008.700>
- Gou B-D, Liu Y, Gao Y-X, Tang K, Zheng L, Zhao Y-D, Zhang T-L (2019) Ex vivo detection of calcium phosphate and calcium carbonate in rat blood serum. *J Struct Biol* 205(1):41–47. <https://doi.org/10.1016/j.jsb.2018.11.010>
- Wu C-Y, Martel J, Young D, Young JD (2009) Fetuin-A/Albumin-mineral complexes resembling serum calcium granules and putative nanobacteria: demonstration of a dual inhibition-seeding concept. *PLoS ONE* 4(11):e8058. <https://doi.org/10.1371/journal.pone.0008058>
- Moe SM, Chen NX (2004) Pathophysiology of vascular calcification in chronic kidney disease. *Circ Res* 95(6):560–567. <https://doi.org/10.1161/01.res.0000141775.67189.98>
- Katsumata K, Kusano K, Hirata M, Tsunemi K, Nagano N, Burke SK, Fukushima N (2003) Sevelamer hydrochloride prevents ectopic calcification and renal osteodystrophy in chronic renal failure rats. *Kidney Int* 64(2):441–450. <https://doi.org/10.1046/j.1523-1755.2003.00126.x>
- Diwan V, Brown L, Gobe GC (2018) Adenine-induced chronic kidney disease in rats. *Nephrology* 23(1):5–11. <https://doi.org/10.1111/nep.13180>
- Viegas CSB, Santos L, Macedo AL, Matos AA, Silva AP, Neves PL, Staes A, Gevaert K, Morais R, Vermeer C, Schurgers L, Simes DC (2018) Chronic kidney disease circulating calciprotein particles and extracellular vesicles promote vascular calcification. *Arterioscler Thromb Vasc Biol* 38(3):575–587. <https://doi.org/10.1161/ATVBAHA.117.310578>
- Chen W, Anokhina V, Dieudonne G, Abramowitz MK, Kashyap R, Yan C, Wu TT, de Mesy Bentley KL, Miller BL, Bushinsky DA (2019) Patients with advanced chronic kidney disease and vascular calcification have a large hydrodynamic radius of secondary calciprotein particles. *Nephrol Dial Transpl* 34(6):992–1000. <https://doi.org/10.1093/ndt/gfy117>
- Akiyama K-i, Miura Y, Hayashi H, Sakata A, Matsumura Y, Kojima M, Tsuchiya K, Nitta K, Shiizaki K, Kurosu H, Kuroso M (2020) Calciprotein particles regulate fibroblast growth factor-23 expression in osteoblasts. *Kidney Int* 97(4):702–712. <https://doi.org/10.1016/j.kint.2019.10.019>
- Bianconi A (1988) XANES Spectroscopy. In: Koningsberger DC, Prins R (eds) X-Ray Absorption: principles, applications, techniques of EXAFS, SEXAFS, and XANES, 92. Wiley, New York,
- Zheng L, Zhao YD, Tang K, Ma CY, Hong CH, Han Y, Cui MQ, Guo ZY (2014) A new experiment station on beamline 4B7A at

- Beijing synchrotron radiation facility. *Spectrochim Acta, Part B* 101:1–5. <https://doi.org/10.1016/j.sab.2014.07.006>
22. Yokozawa T, Oura H, Nakagawa H, Okada T (1982) Adenine-induced hyperuricemia and renal damage in rats. *Nippon Nōgeikagaku Kaishi* 56(8):655–663. <https://doi.org/10.1271/nogeikagaku1924.56.655>
 23. Ferrari P, Singer R, Agarwal A, Hurn A, Townsend MA, Chubb P (2009) Serum phosphate is an important determinant of corrected serum calcium in end-stage kidney disease. *Nephrology* 14(4):383–388. <https://doi.org/10.1111/j.1440-1797.2009.01121.x>
 24. Peng T-C, Gitelman H (1974) Ethanol-induced hypocalcemia, hypermagnesemia and inhibition of the serum calcium-raising effect of parathyroid hormone in rats. *Endocrinology* 94(2):608–611. <https://doi.org/10.1210/endo-94-2-608>
 25. <https://www.taconic.com/rat-model/sprague-dawley> Taconic Biosciences, Inc. (2019).
 26. Vervloet MG, van Ballegooijen AJ (2018) Prevention and treatment of hyperphosphatemia in chronic kidney disease. *Kidney Int* 93(5):1060–1072. <https://doi.org/10.1016/j.kint.2017.11.036>
 27. Bazydło LAL, Needham M, Harris NS (2014) Calcium, magnesium, and phosphate. *Lab Med* 45(1):e44–e50
 28. Danielson BG, Pallin E, Sohtell M (1982) The determination of ultrafiltrable calcium and magnesium in serum. *Upsala J Med Sci* 87(1):43–53. <https://doi.org/10.3109/03009738209178408>
 29. Henderson GS, de Groot FMF, Moulton BJA (2014) X-ray absorption near-edge structure (XANES) spectroscopy. *Rev Mineral Geochem* 78(1):75–138. <https://doi.org/10.2138/rmg.2014.78.3>
 30. Eichert D, Salomé M, Banu M, Susini J, Rey C (2005) Preliminary characterization of calcium chemical environment in apatitic and non-apatitic calcium phosphates of biological interest by X-ray absorption spectroscopy. *Spectrochim Acta B* 60:850–858
 31. Koningsberger DC, Prins R (1988) X-Ray Absorption: Principles, applications, techniques of EXAFS, SEXAFS and XANES, vol 92. *Chemical Analysis*. John Wiley & Sons, New York
 32. Sowrey FE, Skipper LJ, Pickup DM, Drake KO, Lin Z, Smith ME, Newport RJ (2004) Systematic empirical analysis of calcium-oxygen coordination environment by calcium K-edge XANES. *Phys Chem Chem Phys* 6(1):188–192
 33. McDowell H, Brown WE, Sutter JR (1971) Solubility study of calcium hydrogen phosphate. Ion-pair formation *Inorg Chem* 10(8):1638–1643
 34. Pedersen KO (1971) The effect of bicarbonate, P_{CO_2} and pH on serum calcium fractions. *Scand J Clin Lab Invest* 27(2):145–150. <https://doi.org/10.3109/00365517109080201>
 35. de Visscher A, Vanderdeelen J, Königsberger E, Churagulov BR, Ichikuni M, Tsurumi M (2012) IUPAC-NIST Solubility Data Series.95. Alkaline earth carbonates in aqueous systems. Part 1. Introduction, Be and Mg. *J Phys Chem Ref Data* 41(1):013105. <https://doi.org/10.1063/1.3675992>
 36. Bachra BN, Trautz OR, Simon SL (1963) Precipitation of calcium carbonates and phosphates. I. Spontaneous precipitation of calcium carbonates and phosphates under physiological conditions. *Arch Biochem Biophys* 103(1):124–138. [https://doi.org/10.1016/0003-9861\(63\)90018-3](https://doi.org/10.1016/0003-9861(63)90018-3)
 37. Hu Y-B, Wolthers M, Wolf-Gladrow DA, Nehrke G (2015) Effect of pH and phosphate on calcium carbonate polymorphs precipitated at near-freezing temperature. *Cryst Growth Des* 15(4):1596–1601. <https://doi.org/10.1021/cg500829p>
 38. Kosa T, Maruyama T, Otagiri M (1997) Species differences of serum albumins: I. Drug binding sites *Pharm Res* 14(11):1607–1612. <https://doi.org/10.1023/A:1012138604016>
 39. Kosa T, Maruyama T, Otagiri M (1998) Species differences of serum albumins: II. Chem Thermal Stability *Pharm Res* 15(3):449–454. <https://doi.org/10.1023/A:1011932516717>
 40. Kosa T, Maruyama T, Sakai N, Yonemura N, Yahara S, Otagiri M (1998) Species differences of serum albumins: III. Analysis of structural characteristics and ligand binding properties during N-B transitions. *Pharm Res* 15(4):592–598. <https://doi.org/10.1023/A:1011986028529>
 41. Ma GJ, Ferhan AR, Sut TN, Jackman JA, Cho N-J (2020) Understanding how natural sequence variation in serum albumin proteins affects conformational stability and protein adsorption. *Colloids Surf, B* 194:111194. <https://doi.org/10.1016/j.colsurfb.2020.111194>
 42. Poór M, Li Y, Matisz G, Kiss L, Kunsági-Máté S, Kőszegi T (2014) Quantitation of species differences in albumin–ligand interactions for bovine, human and rat serum albumins using fluorescence spectroscopy: a test case with some Sudlow’s site I ligands. *J Lumin* 145:767–773. <https://doi.org/10.1016/j.jlumin.2013.08.059>
 43. Pistolozzi M, Bertucci C (2008) Species-dependent stereoselective drug binding to albumin: a circular dichroism study. *Chirality* 20(3–4):552–558. <https://doi.org/10.1002/chir.20521>
 44. Baird GS (2011) Ionized calcium. *Clin Chim Acta* 412(9–10):696–701. <https://doi.org/10.1016/j.cca.2011.01.004>
 45. Putnam FW (ed) (1975. p.141) *The Plasma Proteins*, vol 1. 2 edn. Academic Press, New York, NY
 46. Majorek KA, Porebski PJ, Dayal A, Zimmerman MD, Jablonska K, Stewart AJ, Chruszcz M, Minor W (2012) Structural and immunologic characterization of bovine, horse, and rabbit serum albumins. *Mol Immunol* 52(3):174–182. <https://doi.org/10.1016/j.molimm.2012.05.011>
 47. Kragh-Hansen U, Vorum H (1993) Quantitative analyses of the interaction between calcium ions and human serum albumin. *Clin Chem* 39(2):202–208
 48. Fanali G, Masi Ad, Trezza V, Marino M, Fasano M, Ascenzi P (2012) Human serum albumin: From bench to bedside. *Mol Aspects Med* 33(3):209–290. <https://doi.org/10.1016/j.mam.2011.12.002>
 49. Pedersen KO (1971) Binding of calcium to serum albumin. I. Stoichiometry and intrinsic association constant at physiological pH, ionic strength and temperature. *Scand J Clin Lab Invest* 28:459–469
 50. Lide DR (2008) *CRC Handbook of Chemistry and Physics*. 88 edn. CRC Press,
 51. Chughtai A, Marshall R, Nancollas GH (1968) Complexes in calcium phosphate solutions. *J Phys Chem* 73(1):208–211
 52. Johnsson MS-A, Nancollas GH (1992) The role of brushite and octacalcium phosphate in apatite formation. *Crit Rev Oral Biol Med* 3(1):61–82
 53. Lim K, Kalim S (2019) The role of nonenzymatic post-translational protein modifications in uremic vascular calcification. *Adv Chronic Kidney Dis* 26(6):427–436. <https://doi.org/10.1053/j.ackd.2019.10.001>
 54. Gajjala PR, Fliser D, Speer T, Jankowski V, Jankowski J (2015) Emerging role of post-translational modifications in chronic kidney disease and cardiovascular disease. *Nephrol Dial Transplant* 30(11):1814–1824. <https://doi.org/10.1093/ndt/gfv048>
 55. Holt SG, Smith ER (2016) Fetuin-A-containing calciprotein particles in mineral trafficking and vascular disease. *Nephrol Dial Transpl* 31(10):1583–1587. <https://doi.org/10.1093/ndt/gfw048>
 56. Kiselev MA, Iua G, Dobretsov GE, Komarova MN (2001) Size of a human serum albumin molecule in solution. *Biofizika* 46(3):423–427
 57. Fernández-Martín JL, Dusso A, Martínez-Cambor P, Dionisi MP, Floege J, Ketteler M, London G, Locatelli F, Górriz JL, Rutkowski B, Bos W-J, Tielemans C, Martín P-Y, Wüthrich RP,

- Pavlovic D, Benedik M, Rodríguez-Puyol D, Carrero JJ, Zoccali C, Cannata-Andía JB (2018) Serum phosphate optimal timing and range associated with patients survival in haemodialysis: the COSMOS study. *Nephrol Dial Transpl* 34(4):673–681. <https://doi.org/10.1093/ndt/gfy093>
58. Isakova T, Xie H, Barchi-Chung A, Smith K, Sowden N, Epstein M, Collerone G, Keating L, Jüppner H, Wolf M (2012) Daily variability in mineral metabolites in CKD and effects of dietary calcium and calcitriol. *Clin J Am Soc Nephrol* 7(5):820–828. <https://doi.org/10.2215/cjn.11721111>
59. Miyagawa A, Tatsumi S, Takahama W, Fujii O, Nagamoto K, Kinoshita E, Nomura K, Ikuta K, Fujii T, Hanazaki A, Kaneko I, Segawa H, Miyamoto K-i (2018) The sodium phosphate cotransporter family and nicotinamide phosphoribosyltransferase contribute to the daily oscillation of plasma inorganic phosphate concentration. *Kidney Int* 93(5):1073–1085. <https://doi.org/10.1016/j.kint.2017.11.022>
60. Peters T Jr (1995) All about albumin: biochemistry, genetics, and medical applications, 1st edn. Academic Press, New York
61. Bern M, Sand KMK, Nilsen J, Sandlie I, Andersen JT (2015) The role of albumin receptors in regulation of albumin homeostasis: implications for drug delivery. *J Control Release* 211:144–162. <https://doi.org/10.1016/j.jconrel.2015.06.006>
62. Levin A, Bakris GL, Molitch M, Smulders M, Tian J, Williams LA, Andress DL (2007) Prevalence of abnormal serum vitamin D, PTH, calcium, and phosphorus in patients with chronic kidney disease: results of the study to evaluate early kidney disease. *Kidney Int* 71(1):31–38. <https://doi.org/10.1038/sj.ki.5002009>
63. Zhang Q, Liu Y, Gou B-D, Zheng L, Gao Y-X, Zhang T-L (2016) Quantitative chemical relations at pseudo-equilibrium in amorphous calcium phosphate formation. *RSC Adv* 6(104):102710–102723. <https://doi.org/10.1039/c6ra21892j>
64. Herrmann M, Schäfer C, Heiss A, Gräber S, Kinkeldey A, Büscher A, Schmitt MMN, Bornemann J, Nimmerjahn F, Herrmann M, Helming L, Gordon S, Jahnen-Dechent W (2012) Clearance of fetuin-A-containing calciprotein particles is mediated by scavenger receptor-A. *Circ Res* 111(5):575–584. <https://doi.org/10.1161/CIRCRESAHA.111.261479>
65. Aghagolzadeh P, Bachtler M, Bijarnia R, Jackson C, Smith ER, Odermatt A, Radpour R, Pasch A (2016) Calcification of vascular smooth muscle cells is induced by secondary calciprotein particles and enhanced by tumor necrosis factor- α . *Atherosclerosis* 251:404–414. <https://doi.org/10.1016/j.atherosclerosis.2016.05.044>
66. Pasch A, Jahnen-Dechent W, Smith ER (2018) Phosphate, calcification in blood, and mineral stress: the physiologic blood mineral buffering system and its association with cardiovascular risk. *Int J Nephrol* 2018:5. <https://doi.org/10.1155/2018/9182078>
67. Tertti R, Harmoinen A, Leskinen Y, Metsärinne KP, Saha H (2007) Comparison of calcium phosphate product values using measurement of plasma total calcium and serum ionized calcium. *Hemodial Int* 11(4):411–416. <https://doi.org/10.1111/j.1542-4758.2007.00210.x>
68. Block GA, Port FK (2000) Re-evaluation of risks associated with hyperphosphatemia and hyperparathyroidism in dialysis patients: recommendations for a change in management. *Am J Kidney Dis* 35(6):1226–1237. [https://doi.org/10.1016/S0272-6386\(00\)70064-3](https://doi.org/10.1016/S0272-6386(00)70064-3)
69. Hawley C (2006) Calcium \times phosphate product. *Nephrology* 11:S206–S208. <https://doi.org/10.1111/j.1440-1797.2006.00645.x>

Publisher's Note Springer Nature remains neutral with regard to jurisdictional claims in published maps and institutional affiliations.

Affiliations

Hong-Xing Fan^{1,2} · Bao-Di Gou³ · Yu-Xi Gao² · Gang Wu¹ · Shu-Hu Liu⁴ · Fan Li⁴ · Tian-Lan Zhang³ 

¹ Department of Preclinical and Forensic Medicine, Baotou Medical College, Inner Mongolia University of Science & Technology, Baotou 014010, People's Republic of China

² CAS Key Laboratory for Biomedical Effects of Nanomaterials and Nanosafety, Institute of High Energy Physics, Chinese Academy of Sciences, 19B Yuquan Road, Beijing 100049, People's Republic of China

³ Department of Chemical Biology, Peking University School of Pharmaceutical Sciences, 38 Xueyuan Road, Beijing 100191, People's Republic of China

⁴ Beijing Synchrotron Radiation Facility, Institute of High Energy Physics, Chinese Academy of Sciences, 19B Yuquan Road, Beijing 100049, People's Republic of China